"Single-tap equalizer for MIMO FBMC systems under doubly selective channels"

Rottenberg, François ; Mestre, Xavier ; Horlin, François ; Louveaux, Jérôme

Abstract

Offset-QAM-based filterbank multicarrier (FBMC-OQAM) modulations are known to progressively loose their orthogonality as the channel gets more selective in time and frequency. The effect of channel frequency selectivity on FBMC-OQAM systems has been extensively studied in the literature. Many compensations methods have been proposed to combat it. However, most of them have a significant implementation complexity and do not take into account the time selective nature of the channel. In this paper, we propose a MIMO equalizing structure for doubly selective channel based on a simple single-tap per-subcarrier decoding matrix. The decoding matrices are designed to minimize the mean squared error of the symbol estimate. This decoder exploits the degrees of freedom offered by the extra antennas at the receiver to compensate for the distortion induced by time and frequency selectivity. Simulation results demonstrate the performance gain of the proposed design with respect to classical desig...

Document type : *Communication à un colloque (Conference Paper)*

SINGLE-TAP EQUALIZER FOR MIMO FBMC SYSTEMS UNDER DOUBLY SELECTIVE CHANNELS

*François Rottenberg[†,**], Xavier Mestre[+], François Horlin[**], Jérôme Louveaux[†]

[†]ICTEAM, Université Catholique de Louvain
[**]OPERA, Université libre de Bruxelles
[+]Centre Tecnològic de Telecomunicacions de Catalunya

ABSTRACT

Offset-QAM-based filterbank multicarrier (FBMC-OQAM) modulations are known to progressively loose their orthogonality as the channel gets more selective in time and frequency. The effect of channel frequency selectivity on FBMC-OQAM systems has been extensively studied in the literature. Many compensations methods have been proposed to combat it. However, most of them have a significant implementation complexity and do not take into account the time selective nature of the channel. In this paper, we propose a MIMO equalizing structure for doubly selective channel based on a simple single-tap per-subcarrier decoding matrix. The decoding matrices are designed to minimize the mean squared error of the symbol estimate. This decoder exploits the degrees of freedom offered by the extra antennas at the receiver to compensate for the distortion induced by time and frequency selectivity. Simulation results demonstrate the performance gain of the proposed design with respect to classical designs.

Index Terms— FBMC-OQAM, MIMO, doubly selective channels, equalizer.

1. INTRODUCTION

Offset-QAM-based filterbank multicarrier (FBMC-OQAM) modulations are seen as an interesting alternative to orthogonal frequency division multiplexing, thanks to its increased spectral efficiency and its good time-frequency localization [1]. One of the drawbacks of FBMC-OQAM occurs when the channel gets strongly selective in time and/or in frequency, which progressively destroys the FBMC-OQAM orthogonality due to inter-carrier interference (ICI) and inter-symbol interference (ISI).

The techniques to deal with channel frequency selectivity have been extensively studied in numerous works, in the SISO case [2–5] and in the MIMO case [6–8]. Most of those approaches are based on the design of multi-tap fractionally spaced equalizers. The work originally devised for the SISO case in [9] and later extended for the MIMO case in [10] proposes instead a parallel multi-stage processing architecture at both sides of the communication link.

Conversely, equalization for time selective channels has only been studied in very few works. In [11] and [12], the authors propose an adaptive equalizer for doubly selective channels, that tracks the channel variations in time. In this paper, we propose a very simple design based on single-tap per-subcarrier decoding matrix, which extends the work of [13, 14] to doubly selective channels. The equalizing matrices are designed to minimize the mean squared error (MSE) of the symbol estimate at each subcarrier and each multicarrier symbol of interest, taking into account a first order approximation of the distortion caused by channel time and frequency selectivity. It is shown that as soon as the receiver has more antennas than the number of transmitted streams, it can tune those extra degrees of freedom to compensate for the channel distortion.

*The research reported herein was partly funded by Fonds pour la Formation à la Recherche dans l'Industrie et dans l'Agriculture (F.R.I.A.) and by the Catalan and Spanish governments under grants 2014SGR1567 and TEC2014-59255-C3-1.

1.1. Notations

Vectors and matrices are denoted by bold lowercase and uppercase letters, respectively (resp.). Superscripts *, ^{T} and ^{H} stand for conjugate, transpose and Hermitian transpose operators. The symbols tr, $\mathbb{E}$, $\Im$ and $\Re$ denote the trace, expectation, imaginary and real parts, respectively. $\jmath$ is the imaginary unit. $\mathbf{I}_N$ denotes the identity matrix of size $N \times N$. $\otimes$ stands for the Kronecker product. Symbol $O(x)$ denotes a matrix of possibly increasing dimensions whose entries remain bounded when $x \to 0$.

2. MSE FORMULATION FOR FBMC-OQAM UNDER CHANNEL FREQUENCY SELECTIVITY

2.1. System Model

A FBMC-OQAM transceiver with N_T transmit antennas and N_R receive antennas is considered, as depicted in Fig. 1. Pure spatial multiplexing is assumed, so that the number of streams is equal to N_T, with $N_R \geqslant N_T$. The number of subcarriers is denoted by $2M$ and the number of real-valued multicarrier symbols is denoted by $2N_s$. The real-valued transmitted symbols, denoted by $\mathbf{d}_{m,l} \in \mathbb{R}^{N_T \times 1}$, are FBMC-OQAM modulated using a prototype pulse $p[n]$ of length $L_p = 2\kappa M$, where κ is the overlapping factor. The transmitted signal $\mathbf{s}[n] \in \mathbb{C}^{N_T \times 1}$ can be written as

$$\mathbf{s}[n] = \sum_{l=0}^{2N_s-1} \sum_{m=0}^{2M-1} \mathbf{d}_{m,l} p_{m,l}[n]$$

for $n = 0, \ldots, (2N_s - 1)M + L_p - 1$ and where $p_{m,l}[n] = \jmath^{l+m} p[n - lM] e^{\jmath \frac{2\pi}{2M} m(n - \frac{L_p - 1}{2})}$. We denote by $\boldsymbol{\mathcal{H}}[b, n] \in \mathbb{C}^{N_R \times N_T}$ the time-variant channel impulse response at sampling instant n and corresponding to delay b. The received signal, denoted by $\mathbf{r}[n]$, is given by

$$\mathbf{r}[n] = \sum_{b=-\infty}^{+\infty} \boldsymbol{\mathcal{H}}[b, n] \mathbf{s}[n - b] + \mathbf{w}[n].$$

where $\mathbf{w}[n] \in \mathbb{C}^{N_R \times 1}$ is additive circularly-symmetric white Gaussian noise with zero mean and variance N_0. The received signal

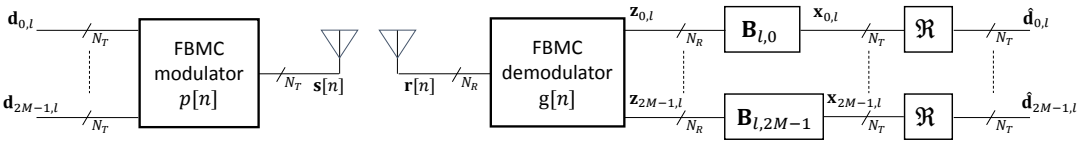

Fig. 1. Classical FBMC-OQAM transceiver.

$\mathbf{r}[n]$ is FBMC-OQAM demodulated using prototype pulse $g[n]$ of length $L_g = 2\kappa M$. The signal after demodulation, at subcarrier l_0 and multicarrier symbol m_0, denoted by $\mathbf{z}_{m_0,l_0} \in \mathbb{C}^{N_R \times 1}$, may be written as

$$\mathbf{z}_{m_0,l_0} = \sum_{n=0}^{L_g-1} \mathbf{r}[n] g^*_{m_0,l_0}[n]$$

where $g_{m,l}[n] = \jmath^{l+m} g[n - lM] e^{\jmath \frac{2\pi}{2M} m(n - \frac{L_g-1}{2})}$. To compensate for the distortion effect of the channel, we use the low complex classical approach, based on a single-tap equalizing matrix $\mathbf{B}_{m_0,l_0} \in \mathbb{C}^{N_T \times N_R}$. The transmitted symbol is then estimated by taking the real part, i.e., $\hat{\mathbf{d}}_{m_0,l_0} = \Re(\mathbf{B}_{m_0,l_0} \mathbf{z}_{m_0,l_0})$. In classical approaches, the channel is assumed not to be very selective and matrix $\mathbf{B}_{m_0,l_0}$ is designed to invert the channel matrix at the subcarrier and multicarrier symbol of interest given by $\mathbf{H}_{m_0,l_0} = \sum_{b=-\infty}^{+\infty} \boldsymbol{\mathcal{H}}[b, l_0 M + \frac{L_g-1}{2}] e^{-\jmath \frac{2\pi}{2M} b m_0}$, which means that we have $\mathbf{B}_{m_0,l_0} \mathbf{H}_{m_0,l_0} = \mathbf{I}_{N_T}$. If the channel is not too selective and for a moderate signal-to-noise ratio (SNR), one can expect to have $\hat{\mathbf{d}}_{m_0,l_0} \approx \mathbf{d}_{m_0,l_0}$.

2.2. MSE Expression Under Strong Channel Selectivity

If the channel is highly selective in time and/or in frequency, the channel variations will break the FBMC-OQAM orthogonality and distortion will be superimposed on the demodulated symbol, mainly due to ICI and ISI. We propose below an approximation of the MSE at the subcarrier m and multicarrier symbol l, that we define as

$$\begin{aligned} \mathrm{MSE}(m,l) &= \mathbb{E}\left(\left\| \hat{\mathbf{d}}_{m,l} - \mathbf{d}_{m,l} \right\|^2 \right) \\ &= P_d(m,l) + P_n(m,l). \end{aligned}$$

We divided the MSE expression into two contributions, namely, the distortion power $P_d(m,l)$ and the noise power $P_n(m,l)$. The distortion term, including the ISI and ICI power, comes from channel selectivity or in other words the fact that the channel is not flat and constant at the subcarrier and multicarrier symbol of interest. The noise term is simply due to the additive noise and is given by (for the receive pulse energy normalized to one)

$$P_n(m,l) = \frac{N_0}{2} \mathrm{tr}\left[\mathbf{B}_{m,l} \mathbf{B}^H_{m,l} \right].$$

Since the noise and symbol samples are uncorrelated, their effect can be studied separately. To propose an analytical and compact approximation of $P_d(m,l)$, we make the following assumptions:

($\mathbf{As1}$) The transmit and receive prototype pulses $p[n]$ and $g[n]$ are of the perfect reconstruction type [15], with energy normalized to one. They are either symmetric or anti-symmetric. Furthermore, $g[n]$ is obtained by the discretization of a smooth real-valued analog waveform $g(t)$ with bounded derivatives, so that

$$g[n] = g\left(\left(n - \frac{2M\kappa - 1}{2} \right) \frac{1}{2M} \right),\ n = 0, \ldots, 2M\kappa - 1.$$

($\mathbf{As2}$) The channel is assumed to be perfectly known by the receiver. To characterize the time variations of the channel, we choose to specify the discrete delay-Doppler spectrum of the channel $\mathbf{P}[b,\nu]$, which equivalently describes $\boldsymbol{\mathcal{H}}[b,n]$:

$$\boldsymbol{\mathcal{H}}[b,n] = \sum_{\nu=-L_\nu}^{L_\nu} \mathbf{P}[b,\nu] e^{\jmath \frac{2\pi}{2N'_s M} n\nu},$$

for $n = 0, \ldots, 2N'_s M - 1$, $b = 0, \ldots, L_b$ with $N'_s = \frac{2N_s + 2\kappa - 1}{2}$. $\mathbf{P}[b,\nu]$ is assumed to be compactly supported in delay and Doppler, i.e., $\mathbf{P}[b,\nu]$ is non zero only for $b = 0, \ldots, L_b$ and $\nu = -L_\nu, \ldots, L_\nu$. Given the maximal delay τ_{max} and maximal Doppler shift f_d of the physical channel, the parameters L_b and L_ν are defined as $L_b = \lfloor \frac{\tau_{max} 2M}{T} \rfloor$ and $L_\nu = \lfloor f_d N'_s T \rceil$ with T being the multicarrier symbol period. Then, we can define the time-variant frequency response of the channel as

$$\mathbf{H}(\omega, t) = \sum_{b=0}^{L_b} \sum_{\nu=-L_\nu}^{L_\nu} \mathbf{P}[b,\nu] e^{-\jmath\omega b} e^{\jmath 2\pi t\nu}$$

given in terms of normalized time and frequency, i.e., $t \in [0,1], \omega \in [0, 2\pi]$. The quantities $\mathbf{H}^{(q,r)}_{m,l}$ are defined as

$$\begin{aligned} \mathbf{H}^{(q,r)}_{m,l} &= \frac{d^q}{d\omega^q} \frac{d^r}{dt^r} \mathbf{H}(\omega, t) \Big|_{\omega = \frac{2\pi}{2M} m, t = \frac{1}{2N'_s M}(lM + \frac{L_g-1}{2})} \\ &= \sum_{b=0}^{L_b} \sum_{\nu=-L_\nu}^{L_\nu} (-\jmath b)^q (\jmath 2\pi\nu)^r \mathbf{P}[b,\nu] e^{-\jmath \frac{2\pi}{2M} mb + \jmath \frac{2\pi}{2N'_s M}(lM + \frac{L_g-1}{2})\nu}, \end{aligned}$$

for $l = 0, \ldots, 2N_s - 1$, $m = 0, \ldots, 2M - 1$. Note that $\mathbf{H}^{(0,0)}_{m,l} = \mathbf{H}_{m,l}$.

($\mathbf{As3}$) The real-valued symbols $\mathbf{d}_{m,l}$ are bounded, independent and identically distributed random variables with zero mean and variance $P_s/2$.

($\mathbf{As4}$) The channel is inverted at the receiver, i.e.,

$$\mathbf{B}_{m,l} \mathbf{H}_{m,l} = \mathbf{I}_{N_T}, \tag{1}$$

for $l = 0, \ldots, 2N_s - 1, m = 0, \ldots, 2M - 1$. This implicitly assumes that the channel $\mathbf{H}_{m,l}$ is full rank.

Under this assumptions, we propose the following approximation of $P_d(m,l)$.

Proposition 2.1. *Under* ($\mathbf{As1}$)-($\mathbf{As4}$), *as* $\frac{\tau_{max}}{T} \longrightarrow 0$, $Tf_d \longrightarrow 0$, *we can write*

$$\begin{aligned} P_d(m,l) = &\frac{\eta_{(0,1),(0,1)}}{(N'_s)^2} tr\left[\left(\mathbf{B}_{m,l} \mathbf{H}^{(0,1)}_{m,l} \right) \left(\mathbf{B}_{m,l} \mathbf{H}^{(0,1)}_{m,l} \right)^H \right] \\ &+ \frac{\eta_{(1,0),(1,0)}}{(2M)^2} tr\left[\left(\mathbf{B}_{m,l} \mathbf{H}^{(1,0)}_{m,l} \right) \left(\mathbf{B}_{m,l} \mathbf{H}^{(1,0)}_{m,l} \right)^H \right] \\ &+ \frac{2\eta_{(0,1),(1,0)}}{2MN'_s} \Im tr\left[\left(\mathbf{B}_{m,l} \mathbf{H}^{(0,1)}_{m,l} \right) \left(\mathbf{B}_{m,l} \mathbf{H}^{(1,0)}_{m,l} \right)^H \right] \\ &+ O\left((\frac{\tau_{max}}{T})^2 \right) + O\left((Tf_d)^2 \right) + O\left(\frac{\tau_{max}}{T} (Tf_d) \right) \end{aligned}$$

where the different η's are pulse related quantities properly defined in the Appendix.

Proof. The MSE approximation is obtained by a first order Taylor approximation of the demodulated signal with respect to the time and frequency variations of the channel. The details of the proof are omitted due to space constraints. □

Note that, the previous expression is an approximation, that holds true asymptotically as $\frac{\tau_{max}}{T} \longrightarrow 0$, $Tf_d \longrightarrow 0$. In practice, T can be both considered large w.r.t. τ_{max} and small w.r.t. f_d such that the approximation is very accurate.

3. DECODER DESIGN TO COMPENSATE FOR THE CHANNEL SELECTIVITY

The goal now is to optimize the above MSE formula to obtain the expression of the optimal decoder in the asymptotic regime. Due to the channel inversion constraint (1), the multi-stream interference is mitigated. The optimal decoder should then compensate for time and frequency selectivity of the channel while keeping the noise level low enough. For the sake of clarity, in the following, the subcarrier and multicarrier symbol indexes will be omitted, such that all time-frequency depending quantities should be understood as evaluated at the subcarrier and multicarrier symbol of interest. The general expression of any decoder that satisfies (1) is given by

$$\mathbf{B} = \mathbf{H}^{\dagger} + \tilde{\mathbf{B}}\mathbf{P}^{\dagger}$$

where $\mathbf{H}^{\dagger} = \left(\mathbf{H}^H\mathbf{H}\right)^{-1}\mathbf{H}^H$, $\mathbf{P}^{\dagger} = \mathbf{I}_{N_R} - \mathbf{H}\mathbf{H}^{\dagger}$ and $\tilde{\mathbf{B}}$ is a matrix left to be optimized. The above expression of $\mathbf{B}$ shows that the optimal decoder can be written as the pseudo inverse of the channel plus a matrix lying on the left null space of $\mathbf{H}$. In the case $N_R = N_T$, it is obvious to see that $\mathbf{B}$ is fixed to the inverse of the channel and there are no extra degrees of freedom. On the contrary, as N_R increases relatively to N_T, there is more and more degrees of freedom left to optimize and one can expect a better compensation of the noise and distortion. Note that the assumption that $N_R > N_T$ makes for instance particular sense in the uplink of cellular networks where the number of base stations could be drastically increased in a massive MIMO scenario [16].

3.1. Decoder Optimization

By using the expression of $P_d(m,l)$ and the approximation of $P_n(m,l)$ derived above, the optimization problem can be formulated as follows,

$$\min_{\tilde{\mathbf{B}}} \mathrm{MSE}(m,l) = \mathrm{tr}\left[\left(\mathbf{H}^{\dagger} + \tilde{\mathbf{B}}\mathbf{P}^{\dagger}\right)\left(\mathbf{\Psi} + \frac{N_0}{2}\mathbf{I}_{N_R}\right)\left(\mathbf{H}^{\dagger} + \tilde{\mathbf{B}}\mathbf{P}^{\dagger}\right)^H\right],$$

where matrix $\mathbf{\Psi}$ is given by

$$\mathbf{\Psi} = \frac{\eta_{(0,1),(0,1)}}{(N_s')^2}\mathbf{H}^{(0,1)}\mathbf{H}^{(0,1)H} + \frac{\eta_{(1,0),(1,0)}}{(2M)^2}\mathbf{H}^{(1,0)}\mathbf{H}^{(1,0)H} + \jmath\frac{\eta_{(0,1),(1,0)}}{2MN_s'}\left(\mathbf{H}^{(1,0)}\mathbf{H}^{(0,1)H} - \mathbf{H}^{(0,1)}\mathbf{H}^{(1,0)H}\right).$$

This problem is a quadratic form in the variable $\tilde{\mathbf{B}}$ which can be easily solved by differentiation with respect to $\tilde{\mathbf{B}}^*$ and setting the derivative to zero. The expression of the optimized decoder is then given by

$$\mathbf{B} = \mathbf{H}^{\dagger}\left(\mathbf{I}_{N_R} - \mathbf{\Psi}\mathbf{P}^{\dagger}\left(\mathbf{\Psi}\mathbf{P}^{\dagger} + \frac{N_0}{2}\mathbf{I}_{N_R}\right)^{-1}\right).$$

3.2. Asymptotic Behavior at Low and High SNR

It is easy to see that at low SNR, i.e., when $N_0 \longrightarrow +\infty$, the optimized decoder converges to the classical pseudo inverse of the channel $\mathbf{B} = \mathbf{H}^{\dagger}$. Indeed, in that regime, the noise power is dominant relatively to the distortion power and the best to do is to invert the channel combining the signals coming from each receive antenna to prevent noise amplification.

As explained above, the distortion will be better compensated as N_R increases. One could be interested to know the number of receive antennas N_R required to completely compensate the distortion caused by the channel selectivity in the high SNR regime, i.e., when $N_0 \to 0$. In [13], it was shown that, when the receiver has twice as many antennas as the number of transmit antennas, it can completely remove the first order approximation of the distortion at high SNR. However, in that work, a quasi-static channel was assumed such that only the effect of frequency selectivity was regarded. Here, the channel time selectivity should also be mitigated.

When $N_0 \to 0$, the MSE is given by the distortion power only, $\mathrm{MSE} = \mathbf{B}\mathbf{\Psi}\mathbf{B}$. Hence, in order to completely remove the first order distortion power, matrix $\mathbf{B}$ should on the one hand satisfy (1) and on the other hand lie in the null space of $\mathbf{\Psi}$. Let us define the i-th decoding vector as $\mathbf{b}_i^H = \mathbf{e}_i^H\mathbf{B}$ where $\mathbf{e}_i$ is the i-th column of the identity matrix $\mathbf{I}_{N_T}$. Vector $\mathbf{b}_i^H \in \mathbb{C}^{1\times N_R}$ should generally satisfy

$$\mathbf{b}_i^H\mathbf{H} = \mathbf{e}_i^H, \mathbf{b}_i^H\mathbf{H}^{(0,1)} = \mathbf{0}, \mathbf{b}_i^H\mathbf{H}^{(1,0)} = \mathbf{0}, \quad i = 1,\ldots,N_T.$$

For this problem to be feasible, N_R has to be larger than the number of linearly independent constraints. We will assume that all matrices are full rank. Depending on the channel selectivity, we differentiate three cases:

- No channel selectivity ($\mathbf{H}^{(0,1)} = \mathbf{H}^{(1,0)} = \mathbf{0}$): in this trivial case, the MSE is zero by assumption ($N_R \geqslant N_T$).
- Channel with frequency or time selectivity only ($\mathbf{H}^{(0,1)} = \mathbf{0}$ or $\mathbf{H}^{(1,0)} = \mathbf{0}$): in that case, at least $2N_T$ receive antennas are required, as was the case in [13].
- Channel with time and frequency selectivity: in that case, at least $3N_T$ receive antennas are required.

4. SIMULATION RESULTS

This section aims at demonstrating the performance of the proposed decoder design with respect to classical designs. By "classical" decoder, we refer to single-tap per-subcarrier decoding matrices that assume a constant and flat channel at the subcarrier level, i.e., the pseudo inverse of the channel, $\mathbf{B}_{m,l} = \mathbf{H}_{m,l}^{\dagger}$. We consider an FBMC-OQAM system with $2M = 128$ subcarriers and a frame transmission composed of $2N_s = 100$ real multicarrier symbols. The subcarrier spacing is fixed to $1/T = 15$kHz as in LTE systems. The transmit and receive pulses are the Phydyas prototype pulse [17]. Note that this pulse is only of the nearly-perfect-reconstruction type and does not fulfill $(\mathbf{As1})$. However, given that it almost fulfills the PR constraints, the approximation of the distortion in Prop. 2.1 will remain very accurate, as will be shown in the following.

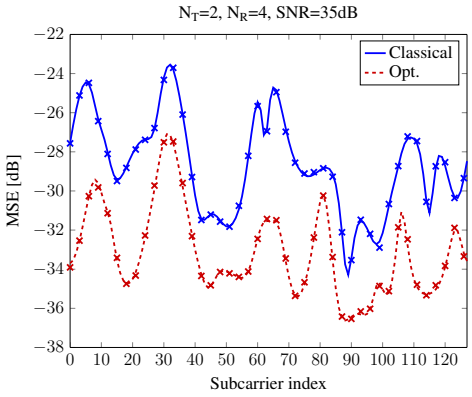

Fig. 2. SNDR at multicarrier symbol $l = 35$ as a function of the subcarrier. Crosses correspond to simulated SNDR and solid/dashed lines to the theoretical proposed approximation.

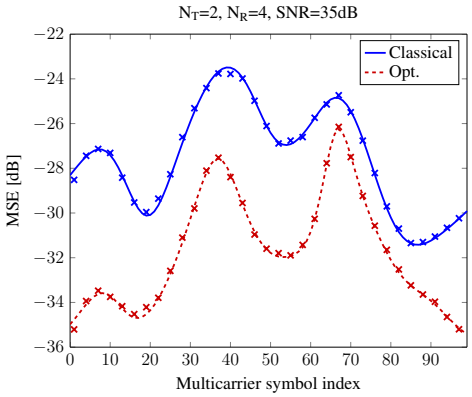

Fig. 3. SNDR at subcarrier $m = 35$ as a function of the multicarrier symbol. Crosses correspond to simulated SNDR and solid/dashed lines to the theoretical proposed approximation.

In the simulations, one channel realization is drawn and the performances are averaged over multiple frame transmission where data and noise samples are regenerated. The SNR of the system is 35dB. The delay-Doppler discrete channel coefficients $\mathbf{P}[b,\nu]$ are assumed zero-mean and independent with variance

$$\mathbb{E}\left(\text{vec}\left(\mathbf{P}[b,\nu]\right)\text{vec}^H\left(\mathbf{P}[b,\nu]\right)\right) = \mathbf{I}_{N_R N_T} p_b^2[b] p_\nu^2[\nu]$$

$$p_b^2[b] = \alpha_b 10^{-2\frac{bT}{\tau_{max}2M}}; \quad p_\nu^2[\nu] = \frac{\alpha_\nu}{\sqrt{1-\left(\frac{\nu}{f_d N_s' T}\right)^2}},$$

which models an exponentially decaying power delay profile and a classical Jake's Doppler spectrum. The constants α_b and α_ν are chosen to normalize $\sum_b p_b^2[b]$ and $\sum_\nu p_\nu^2[\nu]$ to one. In the simulations, we fixed $\tau_{max} = 5\mu s$ and $f_d = 400$Hz.

Fig. 2 and Fig. 3 show the MSE in an $N_R = 4, N_T = 2$ scenario at one subcarrier and one multicarrier symbol respectively. As can be seen, the optimized decoder has a large gain of performance over the classical one. One can further check that the crosses that represent the simulated MSE perfectly match the theoretical one in dashed/solid lines, which validates the accuracy of the approximation of Prop. 2.1.

Fig. 4 plots the cumulative density function (CDF) of the MSE of the classical and optimized decoders. A channel realization for

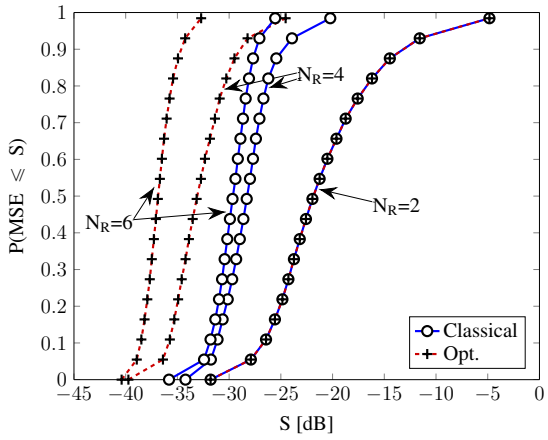

Fig. 4. CDF of the MSE for different number of antennas at the receiver using a classical decoder or the optimized one.

$N_T = 2$ and $N_R = 6$ antennas is drawn and the performance of the receiver using only two, four or all its six antennas is shown. One can check that in the $N_R = N_T = 2$, the performance of the classical and optimized decoders is the same, which is logical since they are the same (no extra degrees of freedom at the receiver). As the number of receive antennas increases, the distortion cannot be compensated for efficiently with a classical decoder while the optimized decoders can use their extra antennas to mitigate the distortion.

5. CONCLUSION

This work investigated the design of equalizers for MIMO doubly selective channels. The proposed design is based on a single-tap per-subcarrier decoding matrix and has a very low complexity. It is shown that, as soon as the receiver has more antennas than the number of streams, these extra degrees of freedom can be used to compensate for the distortion induced by the channel selectivity.

6. APPENDIX

We here define the pulse-related quantities $\eta_{(q_1,r_1),(q_2,r_2)}$ appearing in Proposition 2.1. Given two generic pulses, p, q of length $2M\kappa$ and let $\mathbf{P}$ and $\mathbf{Q}$ denote two $2M \times \kappa$ matrices obtained by arranging the samples of the respective pulses in columns from left to right. We will define

$$\mathcal{R}(p,q) = \mathbf{P} \circledast \mathbf{J}_{2M}\mathbf{Q}$$
$$\mathcal{S}(p,q) = \left(\mathbf{J}_2 \otimes \mathbf{I}_M\right)\mathbf{P} \circledast \mathbf{J}_{2M}\mathbf{Q}$$

where $\circledast$ denotes row-wise convolution, $\otimes$ denotes Kronecker product, $\mathbf{I}_M$ (resp. $\mathbf{J}_M$) are the identity (resp. exchange) matrices of order M. We define $\eta_{(q_1,r_1),(q_2,r_2)}$ as

$$\eta_{(q_1,r_1),(q_2,r_2)} = \frac{P_s M}{2}\text{tr}\Big[\mathbf{U}^+\mathcal{R}\left(p, g^{(q_1,r_1)}\right)\mathcal{R}^T\left(p, g^{(q_2,r_2)}\right) + \mathbf{U}^-\mathcal{S}\left(p, g^{(q_1,r_1)}\right)\mathcal{S}^T\left(p, g^{(q_2,r_2)}\right)\Big]$$

where $\mathbf{U}^\pm = \mathbf{I}_2 \otimes (\mathbf{I}_M \pm \mathbf{J}_M)$ and $g^{(q,r)}[n]$ is defined as the sampling of the function $g^{(q,r)}(t) = \frac{d^q}{dt^q}(t^r g(t))$,

$$g^{(q,r)}[n] = g^{(q,r)}\left(\left(n - \frac{2M\kappa - 1}{2}\right)\frac{1}{2M}\right).$$

7. REFERENCES

[1] Behrouz Farhang-Boroujeny, "OFDM versus filter bank multicarrier," *IEEE Signal Processing Magazine*, vol. 28, no. 3, pp. 92–112, May 2011.

[2] Tero Ihalainen, Tobias Hidalgo Stitz, Mika Rinne, and Markku Renfors, "Channel equalization in filter bank based multicarrier modulation for wireless communications," *EURASIP Journal on Applied Signal Processing*, vol. 2007, no. 1, pp. 140–140, 2007.

[3] D. Waldhauser, L. Baltar, and J. Nossek, "MMSE subcarrier equalization for filter bank based multicarrier systems," in *IEEE 9th Workshop on Signal Processing Advances in Wireless Communications, 2008. SPAWC 2008*. IEEE, 2008, pp. 525–529.

[4] L. Baltar, D. Waldhauser, J. Nossek, et al., "MMSE subchannel decision feedback equalization for filter bank based multicarrier systems," in *IEEE International Symposium on Circuits and Systems, 2009. ISCAS 2009*. IEEE, 2009, pp. 2802–2805.

[5] Aissa Ikhlef and Jérôme Louveaux, "An enhanced MMSE per subchannel equalizer for highly frequency selective channels for FBMC/OQAM systems," in *IEEE 10th Workshop on Signal Processing Advances in Wireless Communications, 2009. SPAWC'09*. IEEE, 2009, pp. 186–190.

[6] Tero Ihalainen, Aïssa Ikhlef, Jérôme Louveaux, and Markku Renfors, "Channel equalization for multi-antenna FBMC/OQAM receivers," *IEEE Transactions on Vehicular Technology*, vol. 60, no. 5, pp. 2070–2085, 2011.

[7] Marius Caus, Ana Pérez-Neira, et al., "Transmitter-receiver designs for highly frequency selective channels in MIMO FBMC systems," *IEEE Transactions on Signal Processing*, vol. 60, no. 12, pp. 6519–6532, 2012.

[8] François Horlin, Jessica Fickers, Thibault Deleu, and Jérome Louveaux, "Interference-free SDMA for FBMC-OQAM," *EURASIP Journal on Advances in Signal Processing*, vol. 2013, no. 1, pp. 1–13, 2013.

[9] Xavier Mestre, Marc Majoral, and Stephan Pfletschinger, "An asymptotic approach to parallel equalization of filter bank based multicarrier signals," *IEEE Transactions on Signal Processing*, vol. 61, no. 14, pp. 3592–3606, 2013.

[10] Xavier Mestre and David Gregoratti, "A parallel processing approach to filterbank multicarrier MIMO transmission under strong frequency selectivity," in *2014 IEEE International Conference on Acoustics, Speech and Signal Processing (ICASSP)*. IEEE, 2014, pp. 8078–8082.

[11] E. Kofidis and A. A. Rontogiannis, "Adaptive BLAST decision-feedback equalizer for MIMO-FBMC/OQAM systems," in *21st Annual IEEE International Symposium on Personal, Indoor and Mobile Radio Communications*, Sept 2010, pp. 841–846.

[12] C. Mavrokefalidis, A. Rontogiannis, E. Kofidis, A. Beikos, and S. Theodoridis, "Efficient adaptive equalization of doubly dispersive channels in MIMO-FBMC/OQAM systems," in *2014 11th International Symposium on Wireless Communications Systems (ISWCS)*, Aug 2014, pp. 308–312.

[13] F. Rottenberg, X. Mestre, and J. Louveaux, "Optimal zero forcing precoder and decoder design for multi-user MIMO FBMC under strong channel selectivity," in *2016 IEEE International Conference on Acoustics, Speech and Signal Processing (ICASSP)*, March 2016, pp. 3541–3545.

[14] F. Rottenberg, X. Mestre, F. Horlin, and J. Louveaux, "Single-Tap Precoders and Decoders for Multiuser MIMO FBMC-OQAM Under Strong Channel Frequency Selectivity ," *IEEE Transactions on Signal Processing*, vol. 65, no. 3, pp. 587–600, Feb 2017.

[15] Pierre Siohan, Cyrille Siclet, and Nicolas Lacaille, "Analysis and design of OFDM/OQAM systems based on filterbank theory," *IEEE Transactions on Signal Processing*, vol. 50, no. 5, pp. 1170–1183, 2002.

[16] E. G. Larsson, O. Edfors, F. Tufvesson, and T. L. Marzetta, "Massive MIMO for next generation wireless systems," *IEEE Commun. Mag.*, vol. 52, no. 2, pp. 186–195, February 2014.

[17] Maurice G Bellanger, "Specification and design of a prototype filter for filter bank based multicarrier transmission," in *IEEE International Conference on Acoustics, Speech, and Signal Processing*. IEEE, 2001, vol. 4, pp. 2417–2420.